Research Article

WIND ENGINEERING

Wind Engineering
2022, Vol. 46(6) 1901–1922

DOI: 10.1177/0309524X221114351
journals.sagepub.com/home/wie
SAGE

Complying the LVRT grid code requirement of a fixed speed wind energy system using unified voltage and pitch angle control strategy

Kanasottu Anil Naik[1], Chandra Prakash Gupta[2] and Eugene Fernandez[2]

Abstract

This paper proposes a Unified Voltage and Pitch angle Control (UVPC) strategy for fixed speed wind farm. The focus put on guaranteeing the LVRT grid code requirement when the wind farm subjected to severe faults. The UVPC consist of static synchronous compensator (STATCOM) voltage control loops with adequate pitch angle control loops which are coordinated to enhance the low-voltage ride-through capability of the wind generators thereby, complying the low voltage ride through (LVRT) grid code requirement as desired by the Germany grid code. Different scenarios such as system without STATCOM and pitch-angle controller, with STATCOM only, and system with STATCOM and pitch-angle control (i.e. UVPC) are simulated. The simulation results show that the adoption of STATCOM and pitch angle controller fulfilling the LVRT grid code requirement to ensure the continuous operation of wind turbines. Furthermore, a concept of critical clearing time (CCT) is discussed and its utility has been emphasized. Calculations, simulations and measurements provide how the increased STATCOM rating can offer an enhanced stability margin.

Keywords

Fault ride through, low voltage ride through, fixed speed, wind turbines, pitch angle controller, STATCOM, three phase faults

Introduction

Wind energy system is one of the renewable energy sources that, at present, experiencing drastic growth due to economical and environmental considerations. Today, more than 341,320 wind turbines are operating all over the world (The Global Wind Energy Council Belgium). The penetration of wind turbines into the utility grid has pressed wind farm operators to perform transient stability analysis before connection to the grid. Thus, a study of the issues related to wind turbine connection to the grid is of paramount importance to the engineers.

However, different countries have the different grid codes, and the performance behavior of wind turbines are monitored by it (Lima et al., 2010). For the wind turbines, the network grid codes have incorporated the requirements such as power quality, voltage control, LVRT, and protection related requirements (Singh and Sundaram, 2021a; Singh et al., 2018, 2019a, 2019d). During contingencies, a critical issue that arises in the power system is voltage collapse, due to weak support of reactive power. Closely related to this issue is low voltage ride through of wind energy systems, which is the most important requirement incorporated in the grid codes. A typical LVRT requirement adopted by the Germany grid code (Lima et al., 2010).

The different types of induction generator based wind energy systems have been studied in De Mello et al. (1982). The modern wind energy systems mostly utilize the variable-speed induction generators. However due to

[1]Department of Electrical Engineering, National Institute of Technology Warangal, Warangal, Telangana, India-506004
[2]Department of Electrical Engineering, IIT Roorkee, Roorkee, Uttarakhand, India-247667

Corresponding author:
Kanasottu Anil Naik, Department of Electrical Engineering, National Institute of Technology Warangal, India-506004.
Email: anilnaik205@nitw.ac.in

their low cost, low maintenance and robustness, the fixed-speed induction generators (FSIGs) are also being used. For example, about 87, 48, and 47.1 MW of installed wind turbines are FSIG based wind turbines in Australia, Germany, and Denmark, respectively (The Wind Power, 2015 These types of induction generators are usually connected at distribution levels or weak nodes where the network has not been originally employed to inject power into the grid (Rathi and Mohan, 2005). Therefore, for ride through severe faults, these wind farms need dynamic reactive power support.

Specially, when the severe fault occurs, the stator terminal voltage of the induction generator drops significantly, causing the electrical torque of the generator to be reduced drastically whereas the mechanical toque is almost constant (Grilo et al., 2007). This condition causes the machine to accelerate, resulting in increased reactive power absorption from the grid. Though the fault is cleared, a large amount of reactive power is drawn by the generator. If the needed amount of reactive power is not available, the machine will cause rotor to accelerate and make rotor speed unstable and get disconnected from the grid.

In order to improve the rotor speed stability margin or to increase critical clearing time of fault, the power compensator devices such as flexible alternative current transmission system (FACTS) are employed to provide adequate amount of reactive power to the induction generators. References Abdel-Baqi and Nasiri (2011) and Tan et al. (1993), employed static var compensator (SVC) for voltage support and transient stability improvement by providing sufficient reactive power to the generator during acceleration. However, STATCOM performs better than the SVC for a given contingency if the same rating devices are considered, especially it exhibits fast response (Molinas and Undeland, 2008). Therefore, in recent time STATCOM has been employed for reactive power compensation of induction generators (Noureldeen et al., 2011; Ramirez et al., 2012; Singh et al., 2006; Suul et al., 2010).

In general pitch angle controller is employed to limit the aerodynamic power at rated value when the wind speed surpasses the rated speed. In addition, it can also improve the transient stability of the wind generator by reducing the mechanical torque with suitable pitch angle generation (Muyeen et al., 2009). Many researchers have carried out their work on transient stability enhancement of wind energy system using pitch angle controller (Duong et al., 2015; Muyeen et al., 2006; Shima et al., 2008; Tamura, 2001; Thet and Saitoh, 2009).

In the above literature some of them (Noureldeen et al., 2011; Ramirez et al., 2012; Singh et al., 2006; Suul et al., 2010) proposed STATCOM to improve wind generator stability and some (Duong et al., 2015; Muyeen et al., 2006; Shima et al., 2008; Tamura, 2001; Thet and Saitoh, 2009) employed pitch controller as it can control the mechanical torque and thus enhances the transient stability of induction generator. But the effectiveness of the simultaneous control of STATCOM and pitch angle controller was not explored. In Chen and Hsu (2008), though the unified voltage source inverter (VSI) and pitch angle control has been proposed to reach effective voltage control and the generator rotor speed stability, but these studies did not evaluate the effect of transient fault condition which is a severe concern to the fixed speed induction generators. A STATCOM and pitch angle control (Zhu and Cao, 2009) are proposed to improve LVRT capability of wind farm subjected to three-phase-to-ground fault. The idea of mixing electrical (e.g. STATCOM) and mechanical (e.g. pitch control system) parts seems to be interesting. But, it does not provide the coordination control of STATCOM in combination with pitch-angle controller for successful LVRT. In this paper, UVPC coordination control strategy has been implemented in which reactive current injected has been controlled through pitch angle blade and STATCOM, and thus improves the low voltage ride through capability and transient stability.

Moreover, the effort was made in the past (Grilo et al., 2007) on stability enhancement of wind turbine driven induction generators assuming the mechanical torque constant during and after the fault which may not be accurate as the mechanical torque depends on the power coefficient and pitch angle. Therefore, in this paper, the accurate mechanical torque versus rotor speed characteristic has been achieved for different pitch angle conditions. Thereafter, transient stability equivalent model of the induction generator has been derived. From which, the analytical results such as generator terminal voltage versus rotor speed and electrical-mechanical torques versus rotor speed are obtained. Finally, how the generator terminal voltage and mechanical torque can be controlled by using STATCOM and pitch angle control, respectively, to improve the LVRT as explained with analytical results.

Modeling of grid connected fixed speed wind energy system

This section provides the information about a typical wind farm power considered and typical LVRT capability requirement of wind generators modeling of wind turbine and its characteristics results, a fixed-speed induction

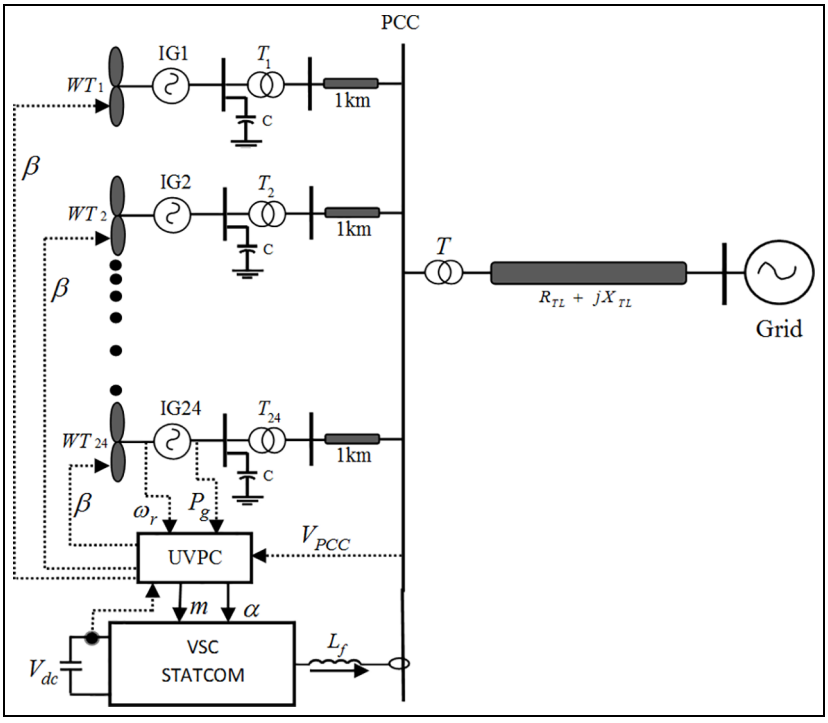

Figure 1. One line diagram of a single FSIG of the typical wind farm.

generator (FSIG) electrical equivalent circuit and modeling, The concept of critical speed, and finally, the effect of pitch angle controller on the critical clearing speed has been discussed.

System configuration

To evaluate the proposed UVPC control strategy, a typical power system is considered as shown in Figure 1. In this paper, 36 MW of wind farm is considered (which consists of twenty-four 1.5 MW induction generators equipped with fixed speed wind turbines) connected to the 120 kV grid. Each induction generator works at the rated operating point and supply 1.5 MW of active power. The stator winding of the each induction generator is connected to the point-of-common-coupling (PCC) through a step-up transformer (0.69/25 kV) which exports power to the 120 kV grid through another step-up transformer T (25/120 kV) and a transmission line. Power factor correction capacitors (C) of 200 kvar are connected to the low voltage terminal of the each wind turbine generators. Under normal operating condition, the capacitors provide required amount of reactive power to the FSIGs. But, these devices fail to provide sufficient reactive power demanded by the FSIGs under severe fault conditions. Therefore, to supply the reactive power and voltage support at the PCC under fault conditions, the STATCOM has been employed and connected to the 25 kV bus.

The addition of STATCOM with appropriate control strategy is expected to increase the stability margin as well as LVRT capability of the wind turbine. Therefore, in this paper UVPC strategy has been proposed to control both mechanical torque (resulting in rotor speed control) and reactive power (resulting in voltage control) of wind energy system using pitch angle controller and STATCOM, respectively.

In general, LVRT can be defined as "the maximum voltage drop (either in terms of magnitude or in terms of time) for which a wind turbine is able to withstand without suffering from rotor speed instability." The Fault ride-through characteristic specified by the Germany grid operator for the wind turbine is shown in Figure 2. According to this grid code requirement, a FSIG is expected to ride-through zero voltage (at the PCC) for 0.15 second due to solid fault, but once the fault is cleared, the connection point voltage must recover to 90% of its nominal value within 1.5 second from the occurrence of fault.

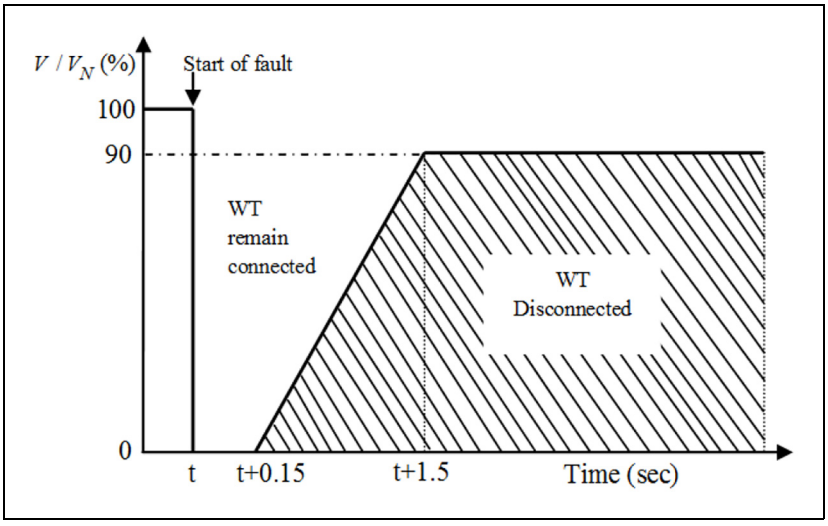

Figure 2. Fault ride-through characteristic specified by the Germany grid operator (Lima et al., 2010).

Modeling of wind turbine

The mechanical power developed by the rotor of a typical wind turbine is directly proportional to the cube of wind speed as:

$$P_m = \frac{1}{2}\rho A_r C_p(\lambda,\beta){V_w}^3 = C_p(\lambda,\beta)P_w \tag{1}$$

where, P_w is available wind power, ρ is the air density (kg/m^3), A_r is the turbine swept area (m^2) and can be written as $A_r = \pi R^2$, C_p is the power coefficient and V_w is the wind speed (m/s).

The typical wind turbine is characterized by the power coefficient (C_p) which depends upon the ratio of rotor-tip speed (λ) and blade pitch-angle (β). In many literatures, the power coefficient curve has been described by different appropriate equations. In this paper, C_p for the studied wind turbine is considered as follows (Ackerman, 2005):

$$C_p(\lambda,\beta) = c_1(c_2/\lambda_i - c_3\beta - c_4)e^{-c_5/\lambda_i} + c_6\lambda \tag{2}$$

where

$$\frac{1}{\lambda_i} = \frac{1}{\lambda + 0.008\beta} - \frac{0.035}{\beta^3 + 1} \tag{3}$$

The coefficients $c_1 - c_6$ are: $c_1 = 0.5176$, $c_2 = 116, c_3 = 0.4$, $c_4 = 5, c_5 = 21$, and $c_6 = 0.0068$ and the blade tip-speed (λ) is defined as:

$$\lambda = \frac{\text{tip speed of the blade}}{\text{wind speed}} = \frac{\omega_r R}{V_w} \tag{4}$$

where, R is the radius of turbine rotor [m] and ω_r is rotor speed [rad/s].

According to equations (1)−(4), the power coefficient versus tip-speed ratio ($C_p - \lambda$) curve for different values of the pitch-angle beta (β) of the studied wind turbine is obtained (Singh and Sundaram, 2021b, 2022; Singh et al., 2019b, 2019c, 2021), as shown in Figure 3. For different values of wind speed (V_w), the turbine output power versus turbine speed characteristics is as shown in Figure 4.

The mechanical power (P_m) shown in equation (1) can be simplified as:

$$P_m = \frac{1}{2}\rho\pi R^2 C_p(\lambda,\beta){V_w}^3 = \frac{1}{2}\rho\pi R^2 C_p(\lambda,\beta)\omega_r^3\left(\frac{R}{\lambda}\right)^3 = C_p(\lambda,\beta)K\omega_r^3 \tag{5}$$

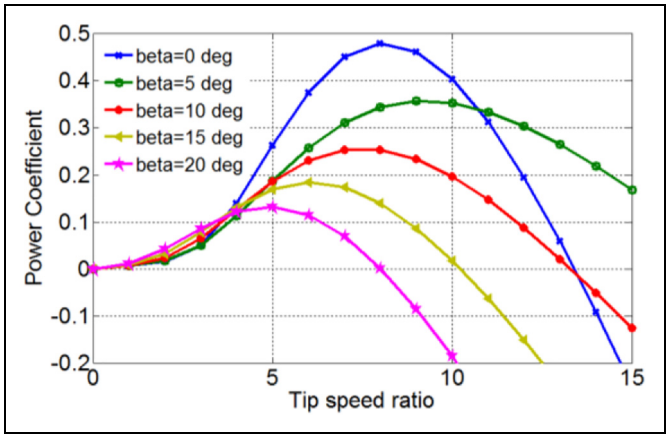

Figure 3. Wind turbine $C_p - \lambda$ curve.

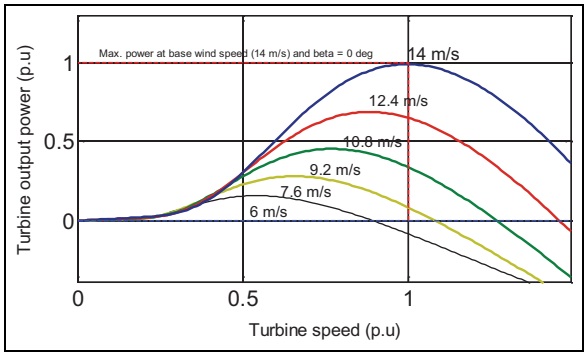

Figure 4. Turbine power characteristics.

where, $K = \frac{1}{2}\rho\pi R^2\left(\frac{R}{\lambda}\right)^3$

Hence, the mechanical torque output of induction generator (IG) can be derived as (Strzelecki and Benysek, 2008):

$$T_m = \frac{P_m}{\omega_r} = \frac{C_p(\lambda,\beta)P_w}{\omega_r} \tag{6}$$

The relation between mechanical torque (T_m) and pitch angle (β) with respect to rotor speed (ω_r) as shown in Figure 5 is obtained using Figure 3 and equation (6). As observed from equation (6), the mechanical power output (P_m) of wind turbine depends upon power coefficient (C_p) and the rotor speed (ω_r) of wind turbine. However, the turbine speed varies very little as the fixed speed cage generators have a speed variation range less than 1% (Wu et al., 2011). Therefore, variation of mechanical power solely depends on power coefficient $C_p(\lambda,\beta)$ which is not constant and varies with tip speed ratio (λ) and pitch angle β. However, in transient stability studies, tip speed ratio variation is very small (Trudnowski et al., 2004). As a result, the mechanical torque mostly depends on the pitch angle (β). So, it can be noticed from Figure 5, the mechanical torque decreases, at the particular point onward of rotor speed, as the pitch angle increases.

Induction generator modeling

In order to obtain the induction generator (IG) model, the network from IG to PCC of the system (see Figure 1) is considered and the corresponding equivalent circuit from IG to PCC is as shown in Figure 6. In this figure, FSIG

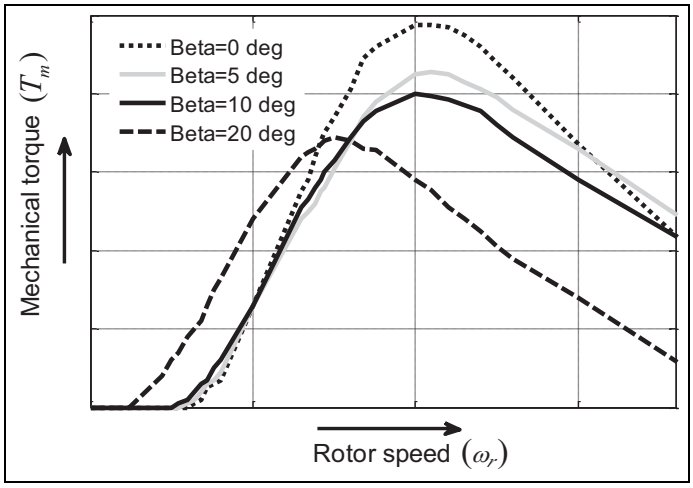

Figure 5. Mechanical torque versus rotor speed.

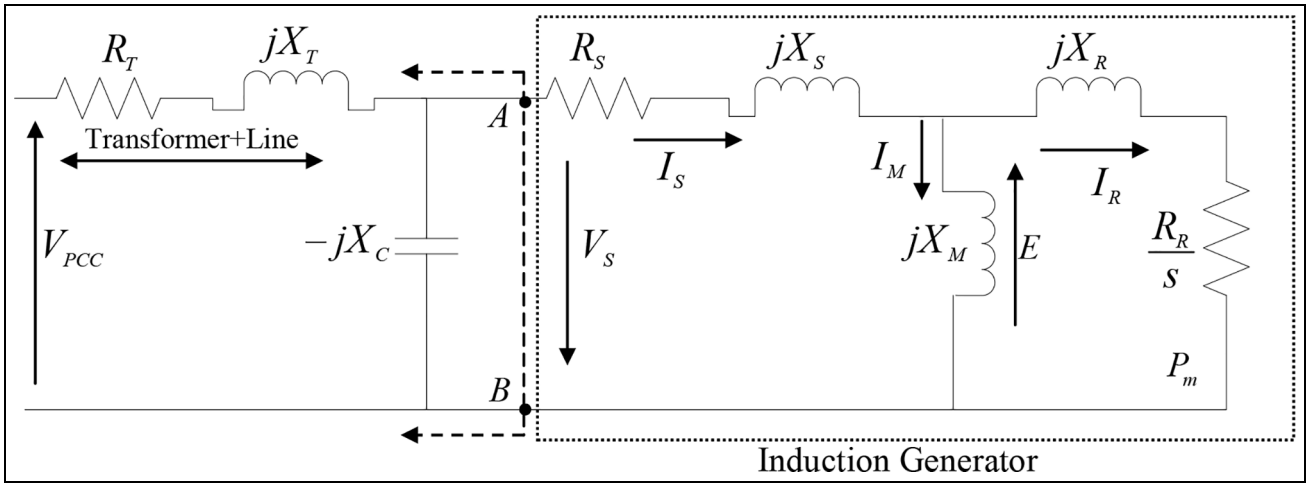

Figure 6. Electrical equivalent of the test system.

is being represented by its steady-state equivalent circuit as shown in Figure 6 inside dotted box, and all the variables and parameters are referred to stator side.

According to the IG equivalent circuit, the mathematical expression for stator terminal voltage (V_S) of FSIG is:

$$V_S = I_S(R_S + jX_S) + E \tag{7}$$

where, E is air gap magnetic field induction electro-magnetic-field (EMF) given by

$$E = jI_M X_M \tag{8}$$

Where X_M magnetizing reactance and I_M is the exciting current of the FSIG. Now the rotor current I_R can be determined from stator current I_S after deducting I_M as follows:

$$I_R = I_S - I_M \tag{9}$$

And then the corresponding mechanical power input to the IG will be given by

$$P_m = 3I_R^2\left(\frac{R_R}{s}\right) \tag{10}$$

Where, R_R and R_S are the rotor and stator resistance, respectively and s is the slip which is less than zero for the IG.

During the stable operation of wind power system, variation in slip is very small and hence voltage equation can be expressed as (Zhang et al., 2009):

$$V_S \approx \frac{I_R}{|s|X_M}K_P \tag{11}$$

where $K_P = \sqrt{X^2 + Y^2}$ with

$$\begin{aligned} X &= -(sX_RR_S + sX_MR_S + X_MR_R + X_SR_R) \\ Y &= R_RR_S - sX_MX_S - sX_MX_R - sX_RX_S \end{aligned} \tag{12}$$

The relation between mechanical to electrical power with efficiency η that:

$$P_m = \eta.P_w \tag{13}$$

From the equation (5) and (10) the rotor current is obtained as:

$$I_R = \sqrt{\frac{\eta C_P(\lambda,\beta)K\omega_r^3 s}{3R_R}} \tag{14}$$

where, the slip (s) is defined as:

$$s = \frac{\omega_s - \omega_r}{\omega_s} \tag{15}$$

where, ω_s is the machine synchronous speed.

From the equations (11), (14), and (15), the stator terminal voltage of the IG (V_S) can be written as:

$$V_S = K_R\sqrt{\frac{\omega_r^3}{|\omega_s - \omega_r|}} \tag{16}$$

where, $K_R = \frac{K_S\sqrt{\omega_s C_P(\lambda,\beta)\eta K}}{\sqrt{3R_R}X_M}$

From equation (16), the behavior of generator terminal voltage of IG (V_S) is as shown in Figure 7, by taking the rotor speed as variable.

It is observed from the Figure 7 that the IG terminal voltage decreases as the rotor speed increases. This is actually the case which occurs when the system subjected to fault. When the severe fault occurs, the stator terminal voltage of the induction generator drops significantly, causing the electrical torque of the generator to be reduced drastically whereas the mechanical toque is almost constant (Grilo et al., 2007). This condition causes the machine to accelerate, causing in dip in the IG terminal voltage (as explained above), resulting in increased reactive power absorption from the grid. Even when the fault is cleared, a large amount of reactive power is still drawn by the generator in order to recover the terminal voltage. If the needed amount of reactive power is not available, the machine will cause rotor to accelerate further and make the rotor unstable and if, this condition is continued for a long time, the IG is disconnected from the grid. Therefore, reactive power compensator (i.e. STATCOM) is needed at the PCC of FSIG in order to supply enough reactive power and consequently, to improve LVRT capability of the FSIG based wind farm.

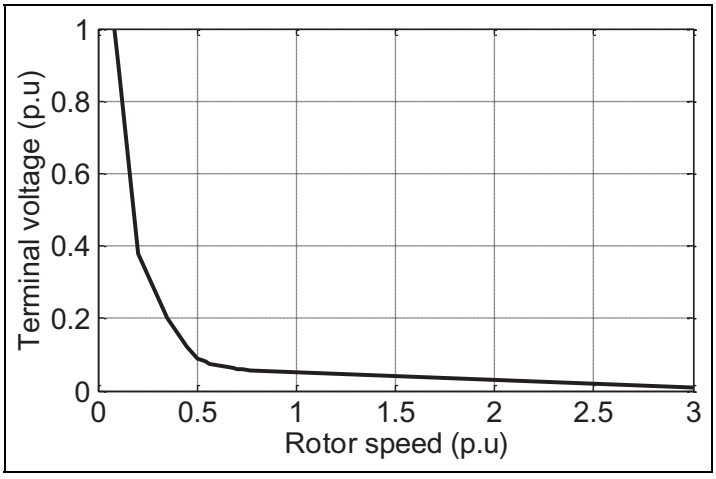

Figure 7. IG terminal voltage versus rotor speed characteristics.

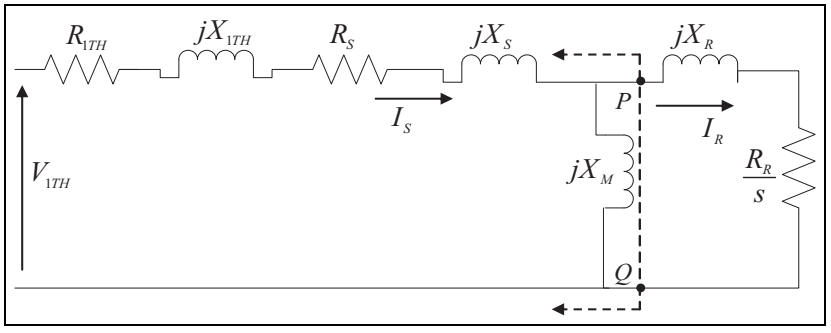

Figure 8. Reduced equivalent circuit of the system.

Concept of critical rotor speed

As discussed above, there would be a critical value for the rotor speed of FSIG, after the occurrence of a fault, above which the rotor may become unstable and cause the disconnection of the IG from the grid. To understand the rotor stability concept of the studied wind energy system, it is required to calculate the electrical torque of the generator from the equivalent circuit of the system shown in Figure 6. From Figure 6, Thevenin equivalent circuit representing the left hand side portion of the equivalent circuit across point A and B, the modified circuit can be shown as given in Figure 8. Where, Thevenin equivalent voltage

$$V_{1TH} = \frac{V_{PCC}(-jX_C)}{R_T + jX_T - jX_C} \tag{17}$$

and the series parameters are:

$$R_{1TH} = R_T \text{ and } X_{1TH} = X_T - X_C \text{ and } X_{1TH} = X_T - X_C$$

From Figure 8, by applying Thevenin concept again at the point P and Q, the further reduced equivalent circuit is obtained as shown in Figure 9.

$$V_{TH} = \frac{V_{1TH}(jX_M)}{R_{1TH} + R_S + jX_{1TH} + jX_S + jX_M} \tag{18}$$

and the equivalent Thevenin resistance and reactance can be obtained as: $R_{TH} = R_{1TH} + R_S$ and $X_{TH} = X_{1TH} + X_S + X_M$.

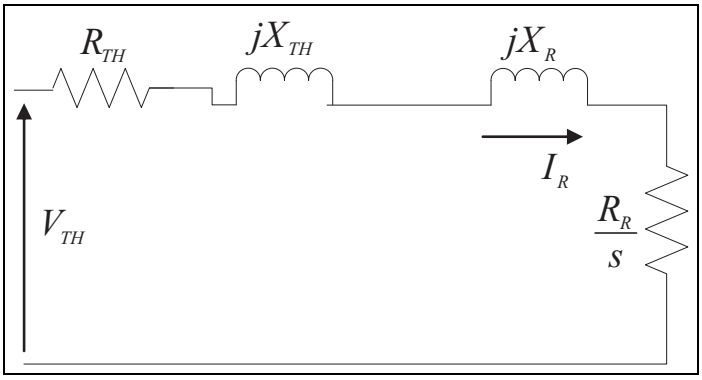

Figure 9. Complete reduced equivalent circuit of the system.

Finally, from the Figure 9, the rotor current can be computed as (Grilo et al., 2007):

$$I_R = \frac{V_{TH}}{\sqrt{(R_{TH} + R_R/s)^2 + (X_{TH} + X_R)^2}} \tag{19}$$

From which, the generator electrical toque can be determined as:

$$T_e = \frac{R_R}{s} I_R^2 = \frac{R_R}{s} \frac{V_{TH}^2}{(R_{TH} + R_R/s)^2 + (X_{TH} + X_R)^2} \tag{20}$$

When the induction machine is operated as generator, the sign convention for the electrical (T_e) and mechanical (T_m) torques are considered as negative. Therefore, the swing equation of a typical IG can be expressed as

$$\frac{d\omega_r}{dt} = \frac{1}{2H}(T_e - T_m) \tag{21}$$

where, H is the inertia constant of the IG. Equation (21) shows that for the IG to be stable, T_e must be greater than T_m, as well T_e equal to T_m at an operating (equilibrium) point which implies that the intersection point of the T_e versus rotor speed (ω_r) and T_m versus rotor speed drawn on a same graph will provide a corresponding stable operation point for the IG. So, using equations (6) and (20), the mechanical and electrical torques versus rotor speed characteristics can be plotted as shown in Figure 10. For better visualization, the mechanical and electrical torques were multiplied by -1.

As observed from Figure 10, let the IG is being at an operating point K, now the occurrence of fault at time t_0, the electrical torque (T_e) suddenly reduces to zero and operating point of the generator shifted from K to M where the rotor speed is ω_0. Due to which, the excess mechanical torque (T_m) with no pitch angle control (i.e. $\beta = 0$) causes the IG rotor to accelerate as governed by the equation (21) and start increasing (during the fault curve). At the instant t_N, the fault is cleared and operating point of the generator shifted to point N where, the T_e is greater than T_m causing the net torque $(T_e - T_m)$ to be negative which causes the rotor speed to decrease and therefore, it eventually leads the generator to return back to its initial operating point K. This clearly shows that the IG will be stable as long as the fault is cleared before a critical speed ω_{crit}.

Effect of pitch angle control

In case, the fault is not cleared before time t_{crit} (corresponding to critical rotor speed ω_{crit}), the rotor speed ω_r will increase further. If the fault is cleared at t_P the operating point of generator T_e is shifted to point P where the T_m greater than T_e thus, the net torque $(T_e - T_m)$ is positive, which results in increase of rotor speed and thus, generator will become unstable. In this condition, it observed from the Figure 10 that by increasing of pitch angle by $\beta = 20^\circ$, the mechanical torque gets reduced below the electrical torque and system retains its stability, thus, the intersection of T_e and T_m at point O provides the new critical speed ($\omega_{crit}new$). It clearly shows that by increasing

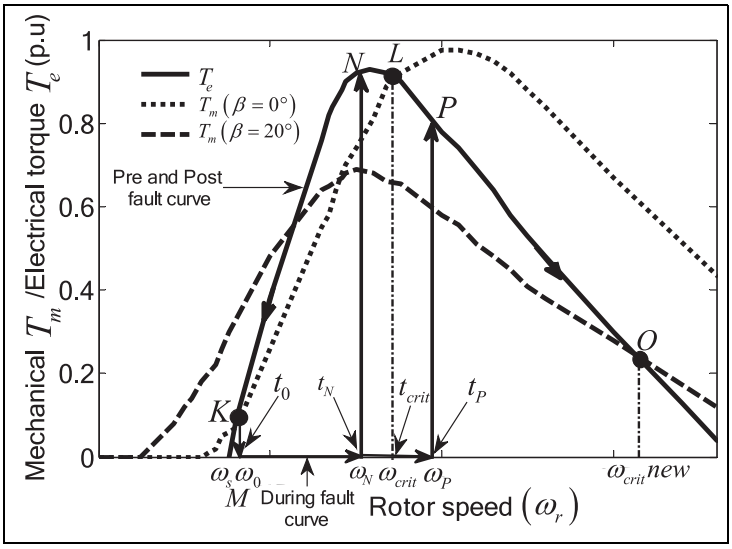

Figure 10. Characteristics of T_e and T_m versus rotor speed.

the pitch angle with the help of wind turbine pitch angle controller, the critical speed can be raised from ω_{crit} to $\omega_{crit}new$. Thus, the stable operation of the system can also maintain over the higher rotor speeds (upto $\omega_{crit}new$).

The critical fault clearance time can be determined, by solving the equations (20) and (21) at these equilibrium points as follows:

$$\left(R_{TH}^2 + (X_{TH} + X_R)^2\right)s^2 + \left(2R_R R_{TH} - R_R V_{TH}^2/T_m\right)s + R_R^2 = 0 \tag{22}$$

which is a second order equation. Now, solving equation (22) and using (15), the steady-state initial rotor speed ω_0 and critical rotor speed ω_{crit} can be determined as

$$\omega_0 = 1 - \frac{b + \sqrt{\Delta}}{2a} \tag{23}$$

$$\omega_{crit} = 1 - \frac{b - \sqrt{\Delta}}{2a} \tag{24}$$

Where $\Delta = b^2 - 4ac$, $a = R_{TH}^2 + (X_{TH} + X_R)^2$, $b = 2R_R R_{TH} - R_R V_{TH}^2/T_m$, and $c = R_R^2$

Substitute the equation (23) and (24) in equation (21) and integrating both side, the expression for the critical clearing time is

$$t_{crit} = \left(\frac{-2H}{T_m}\frac{1}{R_{TH}^2 + (X_{TH} + X_R)^2}\right) \times \left(\sqrt{\frac{R_R^2}{T_M^2}}\left(-4(X_{TH} + X_R)^2 T_m^2 - 4R_{TH}V_{TH}^2 T_m + V_{TH}^4\right)\right) \tag{25}$$

Equation (24) and (25) show that both ω_{crit} and t_{crit} can be increased by reducing the mechanical torque (T_m) developed by the wind turbine by increasing the pitch angle (β).

The unified voltage and pitch angle control (UVPC)

As discussed in above subsection it can be mentioned that if reactive power compensator like STATCOM is installed at the PCC, the required amount of reactive power to the IG can be supplied during and after a fault, resulting in voltage recovery at the PCC. Moreover, it can also improve the LVRT capability of the wind power system, if rating of the STATCOM is increased (Molinas and Undeland, 2008). Furthermore, as explained in

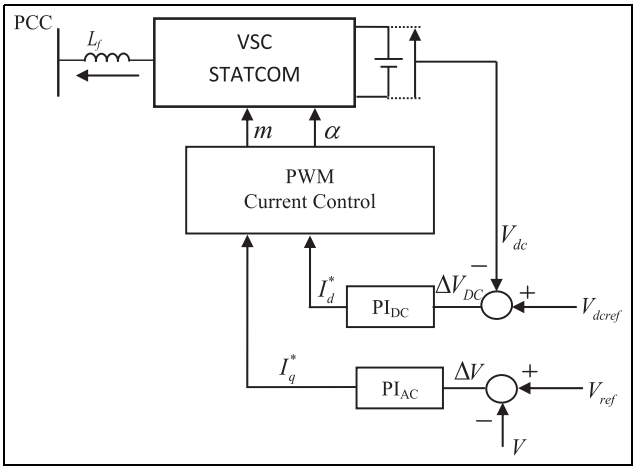

Figure 11. Control scheme of STATCOM.

aforementioned subsection, the fault ride through (FRT) capability of the generator can also be enhanced by decreasing the mechanical torque of the IG by increasing the pitch angle of the associated wind turbine. Therefore, in this paper, for successful LVRT capability of the wind farm simultaneous control of STATCOM and pitch angle controller has been achieved through a coordination control (i.e. UVPC) as explained below:

The STATCOM control scheme

A typical STATCOM is modeled as shown Figure 11, which includes a voltage source converter (VSC), a coupling transformer and the associated control system.

For maintaining the voltage at PCC constant, the AC line voltage (V) is compared with the reference voltage (V_{ref}) and the error/deviation (ΔV) is processed through the controller PI_{AC}. The AC voltage error (ΔV) at the n^{th} instant is

$$\Delta V_{(n)} = V_{ref} - V_{(n)} \tag{26}$$

where, $V_{(n)}$ is the magnitude of the sensed three phase voltages at the PCC at n^{th} instant, V_{ref} is the amplitude of the reference voltage.

For an AC voltage control loop, the controller (PI_{AC}) output (I_q^*) determines the amount of reactive power to be generated by STATCOM. The voltage regulation controller (PI_{AC}), which reacts to a sudden voltage variation and inject the appropriate amount of reactive power, and therefore it is well adapted for system disturbances. The AC voltage controller (PI_{AC}) output ($I_{q(n)}^*$) at n^{th} sampling to regulate the PCC voltage can be expressed as

$$I_q^*(n) = I_q^*(n-1) + K_{Pac}\{\Delta V_{(n)} - \Delta V_{(n-1)}\} + K_{Iac}\Delta V_{(n)} \tag{27}$$

where, K_{Pac} and K_{Iac} are the proportional and integral gain constants of the AC voltage controller, $\Delta V_{(n)}$ and $\Delta V_{(n-1)}$ are the error voltages at the n^{th} and $(n-1)^{th}$ instant and $I_q^*(n-1)$ is the quadrature components of the reference current at the $(n-1)^{th}$ instant.

At the same time, in order to support the DC bus of STATCOM, DC bus voltage (V_{dc}) is also compared with the reference DC voltage (V_{dcref}) and the error voltage (ΔV_{DC}) is passed through another controller PI_{DC}. The output (I_d^*) of this controller determine the source current active power component so that no real power injection is made by STATCOM at the PCC. Similarly, the DC bus voltage error (ΔV_{DC}) at n^{th} sampling is

$$\Delta V_{DC(n)} = V_{dcref} - V_{dc(n)} \tag{28}$$

where, $V_{dc(n)}$ is the sensed DC link voltage of the STATCOM at the n^{th} instant and V_{dcref} is the reference DC voltage. The output of the PI_{DC} controller is to support the STATCOM DC voltage at the n^{th} sampling and expressed as

$$I_d^*(n) = I_d^*(n-1) + K_{Pdc}\{\Delta V_{DC(n)} - \Delta V_{DC(n-1)}\} + K_{Idc}\Delta V_{DC(n)} \tag{29}$$

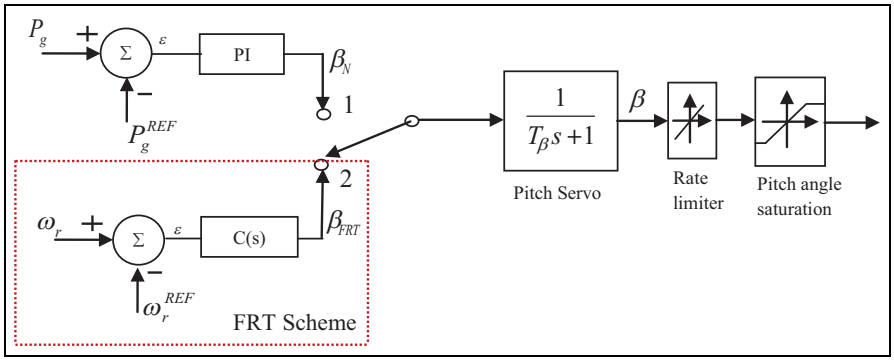

Figure 12. Pitch angle controller strategy.

Where $I_d^*(n)$ and $I_d^*(n-1)$ are the active power components of the source current at the n^{th} and $(n-1)^{th}$ instant. K_{Pdc} and K_{Idc} are the proportional and integral gain constants of the DC voltage controller. Two PI controllers gains (K_{Iac}, K_{Pdc} and K_{Idc}) of the STATCOM are obtained at a specific operating point. Detailed STATCOM control scheme is available in Singh et al. (2006).

Pitch angle control scheme

The main purpose of the pitch angle controller is to maintain the output power of the wind generator at rated value when the wind speed exceeds the rated speed. In addition, it can also improve the transient stability of the wind turbine generator. Specially, for improving the fault-ride-through (FRT) capability of wind generators, the pitch-angle is modified with the help of pitch angle controller as shown in Figure 12 based on generator rotor speed as explained in section 2.5. The inputs to the pitch angle controller are generator rotor speed (ω_r) and the reference rotor speed (ω_r^{REF}). The resulting error (ε) passes through the controller $C(s)$ and thus can improve the transient stability (Duong et al., 2015; Muyeen et al., 2009).

The operating modes (for normal and fault-ride-through operations) of the controller can be determined using selection switch as shown in Figure 12. If the system voltage goes below threshold (i.e. below 90% of nominal voltage V_N) due to severe network faults, the switch connects to position "2" and fault ride through (FRT) scheme of pitch angle controller is activated which generates the pitch angle accordingly to reduce the mechanical torque for preventing generator rotor from over speeding and transient voltage instability. Under normal operating condition, the switch move from "2" to "1" position activating the normal pitch-angle control scheme.

The proposed UVPC scheme

Figure 13 depicts a proposed unified control scheme (dotted box) comprising of pitch angle and voltage control loops. During the disturbances, the STATCOM voltage control loops especially, AC voltage controller provides reactive power compensation whereas, the FRT pitch-angle control loop prevents the rotor acceleration by reducing the mechanical torque. Therefore, the LVRT capability has achieved with reactive current injected by controlling the rotor blade pitch angle and the STATCOM.

The major features of the UVPC can be summarized as:

1) Voltage restoration is essential for the fault-ride-through of a wind generator during faults, which is achieved by injecting quadratic current, determined by AC voltage control loop, into the system.
2) For the severe faults, the fault-ride-through (FRT) scheme of pitch-angle-control loop limits the rotor from over speeding by reducing the wind turbine mechanical power through a suitable pitch angle generation. As a result, the AC voltage control loop can more effectively restore the PCC voltage to satisfy the grid code compliances.
3) After the fault has been cleared (i.e. during normal operating condition), AC voltage control loop can effectively regulate the bus voltage fluctuations. Thus, the active power imbalance of the IG is minimized and the mechanical power and the rotor speed can be more effectively controlled by pitch-angle control with the help of normal pitch-angle-controller.

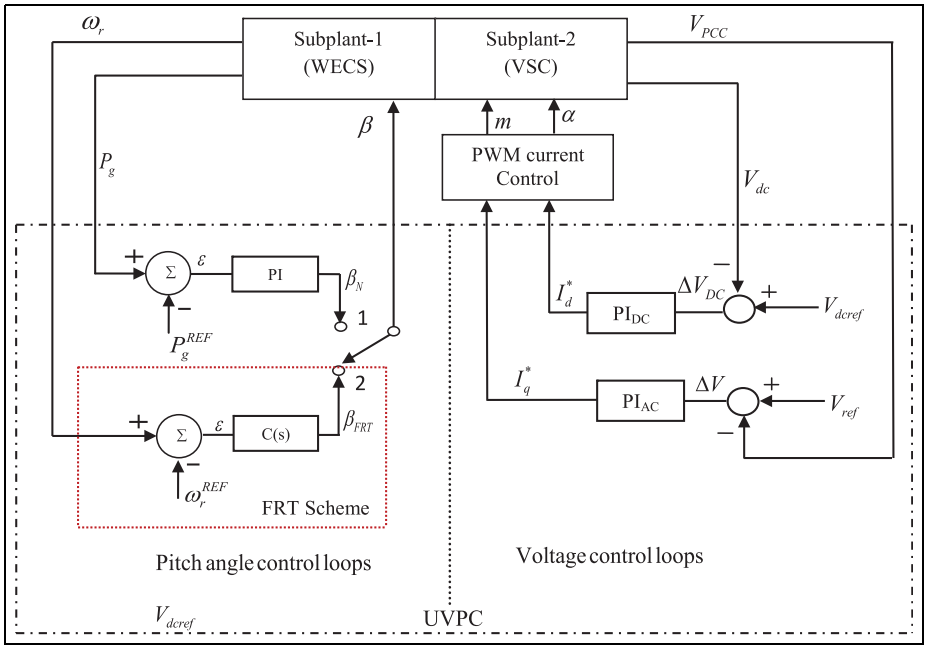

Figure 13. Block diagram of proposed UVPC.

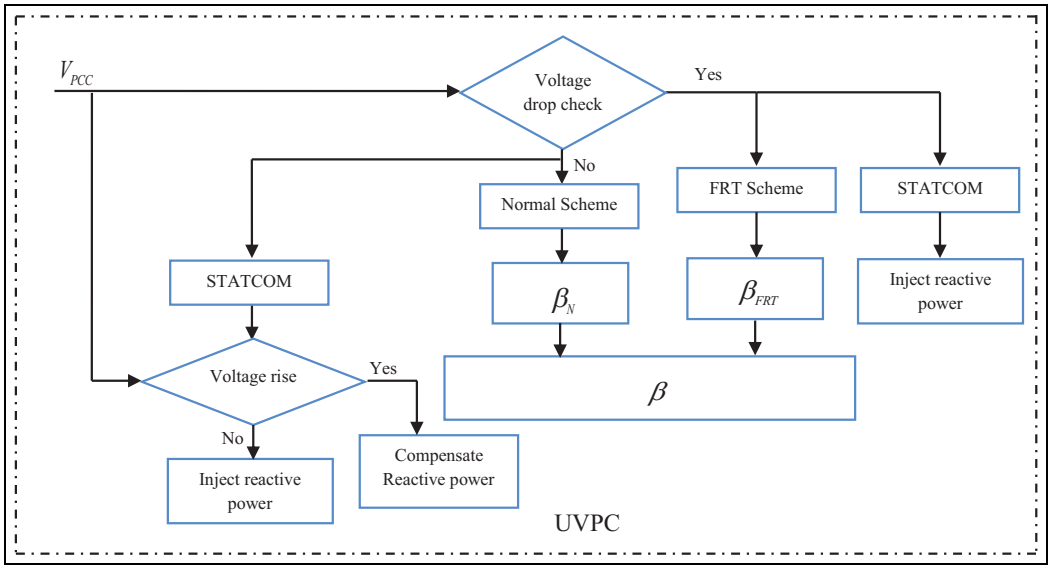

Figure 14. Coordination cycle of UVPC.

The flowchart for simultaneous control of pitch angle and STATCOM (i.e. UVPC) is as shown in Figure 14. The steps of UVPC coordination control algorithm are as follows:

Step 1: From the simulation of faulted system, the value of PCC voltage (V_{PCC}) is determined and checked whether, there exists a severe voltage depression that is, less than nominal operating voltage (V_N).
Step 2: If the condition ($V_{PCC} < 0.9V_N$) is satisfied (especially in case of transient faults), both AC voltage control loop of STATCOM as well as FRT scheme of pitch-angle control loop are activated. The output (I_q^*) of voltage controller (PI_{AC}) determines the amount of reactive power injected into the system, at the same time,

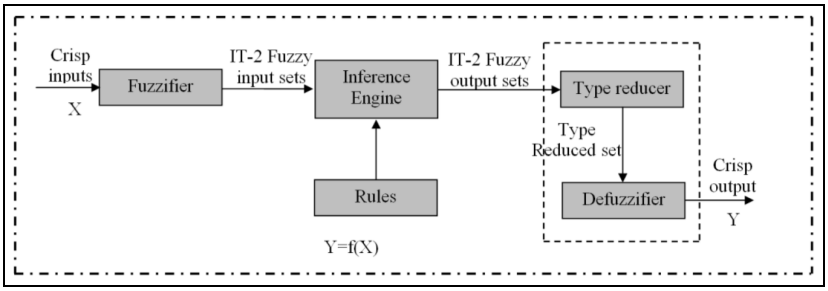

Figure 15. Schematic diagram of type-2 FLC.

the error (ε) in generator rotor speed passes through the controller $C(s)$ which generates an appropriate pitch-angle (β_{FRT}) to reduce the mechanical torque.

Step 3: If the condition ($V_{PCC} < 0.9V_N$) is not satisfied that is, during normal operating condition, if the system voltage and active power fluctuates due to normal disturbances (not severe). In that case, normal pitch-angle control loop determines the pitch angle (β_N) to control the mechanical power thereby reducing the oscillations in the active power. Meanwhile, AC voltage control loop also regulate the voltage at the PCC by injecting/absorbing the necessary reactive power by an appropriate output (I_q^*) through controller ($\mathrm{PI_{AC}}$).

In order to achieve the successful LVRT capability and transient stability enhancement of the wind farm, the pitch angle and voltage control loops of UVPC need to be designed with an effective control method. Generally, STATCOM voltage control and normal pitch-angle loops are designed using conventional PI controller technique, offering satisfactory performance. But, PI controller is not a good choice in fault-ride-through (FRT) scheme of pitch-angle control loop, as the controller is required to generate a desired pitch-angle command (β_{FRT}) so that the mechanical power can be reduced in a very efficient manner to limit rotor speed. Therefore, fuzzy logic controller (type-1) is the best choice for FRT scheme of pitch-angle controller (Duong et al., 2015). However, once the membership functions are defined for designing the controller, the uncertainties in membership functions (MFs) cannot be incorporated, thereafter (Hagras and Wagner, 2012; Mendel, 1999). This may degrade the controller performance especially, when the wind farm is subjected to severe disturbances. In such conditions, an advanced type-2 fuzzy logic controller is a better choice in comparison of their traditional fuzzy logic counterpart (type-1) (Mendel et al., 2006; Qilian and Mendel, 2000). The following subsections, therefore, discuss the designing of the interval type-2 FLC for the FRT scheme of pitch-angle controller.

An interval type-2 fuzzy logic controller (FLC)

A typical Interval Type-2 FLC consists of two membership functions—primary and secondary. The primary membership grade of a type-2 FLC is a normal fuzzy set in [0, 1] whereas, the secondary membership is a crisp number in [0, 1] (Mizumoto and Tanaka, 1976). Furthermore, the secondary membership function and the range of uncertainty are decided by the third dimension of type-2 fuzzy sets and footprint-of-uncertainty (FOU), respectively. Thus, in designing the type-2 FLC, these features can offer additional degree-of-freedom to handle various uncertainties. Hence, wind energy systems, being highly uncertain, can utilize the special features of type-2 FLCs to improve its operational efficiency during the grid interaction. Figure 15 shows the steps involved in the type-2 FLC design algorithm.

As observed from Figure 15, first-of-all, the crisp inputs are converted into fuzzy inputs using type-2 membership functions to account for the uncertainties involved in the expert knowledge. Then using logical operators, a set of fuzzy rules is framed to combine the fuzzy output sets into a single set using the inference mechanism. Afterward, using the type reduction operation, the output of inference engine is converted to type-1 fuzzy set and then, the crisp output is obtained from type-reduced set using various defuzzification methods as done in case of the conventional type-1 FLC. To achieve fast and accurate mechanical torque control during the network disturbances, the FRT scheme of the UVPC is designed using type-2 fuzzy logic controller and the proposed structure is as shown in Figure 16.

The controller gains K_e and K_d are used as a scaling gains for input signals whereas, K_u is used for scaling the output signal. These scaling gains can be variables or constants. During the FLC design, these can play an

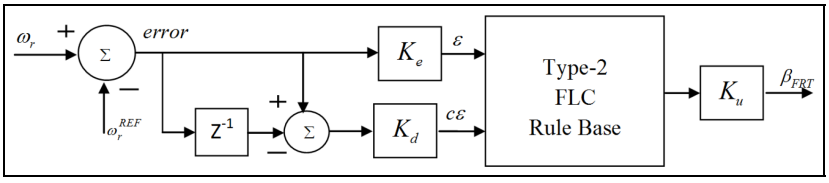

Figure 16. Proposed structure of type-2 FLC for FRT scheme of UVPC.

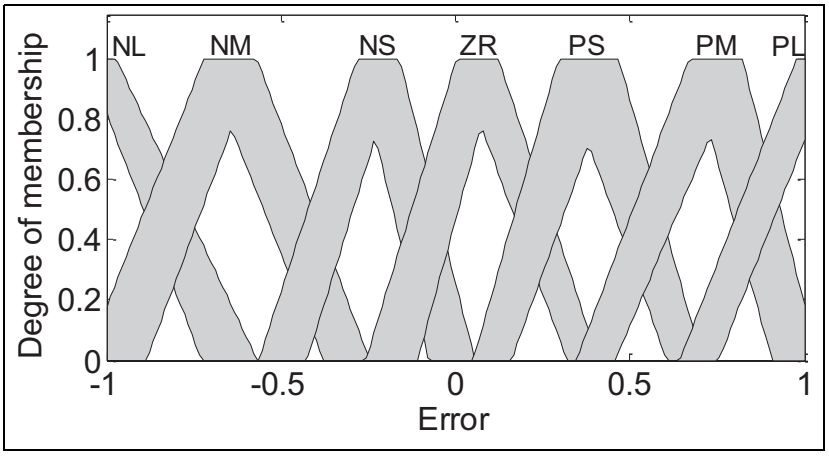

Figure 17. Type-2 FLC designed membership function.

Table 1. FRT controller rules.

Change in Error ($c\varepsilon$)	Error (ε)						
	NL	NM	NS	ZR	PS	PM	PL
NL	NL	NL	NL	NL	NM	NS	ZR
NM	NL	NL	NL	NL	NS	ZR	PS
NS	NL	NL	NM	NM	ZR	PS	PM
ZR	NL	NM	NS	ZR	PS	PM	PL
PS	NM	NS	ZR	PM	PM	PL	PL
PM	NS	ZR	PS	PM	PL	PL	PL
PL	ZR	PS	PM	PL	PL	PL	PL

important role to achieve suitable steady-state and transient-state responses. In this work, these gain constants are chosen by trial-and-error approach.

The controller error (ε) and change in error ($c\varepsilon$) signals as shown in Figure 16 are fuzzified by employing seven triangular linguistic variables of MFs of type-2 FLCs are as shown in Figure 17. Notation for the fuzzy sets as: PL (Positive Large), PM (Positive Medium), PS (Positive Small), ZR (Zero), NS (Negative Small), NM (Negative Medium), NL (Negative Large). These MFs are chosen, based on prior knowledge and observations from the various simulation results. For all the inputs and outputs, the universe-of-discourse is chosen as $[-1, +1]$.

The major function in the inference engine is the rules' implementation, aggregation and type reduction. With help of the experts' knowledge on the controllers, a control strategy framed as a set of IF-THEN rules and is as: If (ε is x_1) and ($c\varepsilon$ is y_1) then (β_{FRT} is w_1).

Similarly, 49 inference rules were defined for all input-output MFs as shown in Table 1. In the type-2 FLCs, the union and intersection functions are defined by join and meet operations to map the input and output sets with fired rules. A detailed mathematical relation between the meet and join operations has been presented in

(Mizumoto and Tanaka, 1976). During the aggregation operation, all the fired rules are converted to become a single output fuzzy set. However, due to computational limitations the output of inference engine cannot be converted directly to crisp value. Thus, type reduction (TR) method has been suggested in the type-2 FLC system to obtain type-1 fuzzy sets from type-2 output fuzzy sets, and later the normal defuzzification techniques can be applied. Height, center-of-sets, center-of-sums, and modified-height are the most accepted TR methods (Karnik and Mendel, 1999), in which centroids of the embedded type-2 sets are calculated.

The common defuzzification methods used for the type-2 FLC are the first (or last) of maxima, centroid-of-area and mean-of-max methods. In this study, centroid-of-area method has been utilized which is the most reasonable and popular method among the others. The centroid of the type-2 fuzzy set is the collection of centroids of all of its embedded sets. The defuzzification method converts the output fuzzy into crisp value.

Results and discussions

In order to observe the LVRT capability enhancement by the proposed UVPC, a solid three-phase-fault (with duration of 150 ms) is applied at the PCC of the wind farm in the test system (as shown in Figure 1) at $t = 10$ seconds. To evaluate the effectiveness of UVPC strategy, three cases are considered: (1) System without STATCOM and pitch-angle controller (2) System with STATCOM only and (3) System with STATCOM as well as pitch-angle control (i.e. UVPC). The results are as follows:

Case 1: Without STATCOM and pitch-angle controller

In this case, the wind power system is considered (without STATCOM and pitch angle control) which is subjected to a three-phase fault at the PCC, for duration of 150 ms at time $t = 10$ seconds. Figure 18(a) to (e) shows the various responses of the system.

When the fault occurs, the electrical torque of the generator reduces drastically whereas the mechanical-input torque remains constant as shown in Figure 18(a), due to this difference between the electrical and mechanical torque, the generator rotor speed start increases as governed by the equation (21) as shown in Figure 18(b). Since the electrical torque decreases due to fault, the real power output of the generator also reduces accordingly as shown in Figure 18(c). Thereafter, it reduces to zero at 13 second and becomes negative, resulting in the motoring action of the FSIG which can damage the turbine blades, if the protection system does not employed. As observed from Figure 18(d), before the fault (under normal operating condition) FSIG draws around 5 Mvar from the grid. After the fault is cleared, the induction generator absorbs a large amount of reactive power, impeding the voltage restoration at PCC. But, due to lack of quick reactive power supply, the PCC voltage cannot be fully retrieved (not able to recover upto 90%) as shown in Figure 18(e). Consequently, it increases rotor speed further as shown in Figure 18(b), and wind farm even consumes large amount of reactive power around 22 Mvar as shown in Figure 18(d). This process may lead to power system instability, and therefore, FSIG may be tripped off from the grid by the over-speed protection. Under this condition, the FSIG does not possess sufficient ride-through capability on its own and therefore, installation of STATCOM may be justified at the PCC to improve its ride-through capability.

Case 2: System with STATCOM

As discussed above, in order to improve system stability, a reactive power compensator (i.e. STATCOM) is installed at the PCC and considering the same solid three phase fault as before. The system responses are as shown in Figure 19(a) to (f).

It is observed from Figure 19(a) that as the fault occurs at 10 seconds, the electrical torque reduced to zero and the mechanical torque remains (assumed as constant) exist, and therefore, the rotor speed of FSIG increases as shown in Figure 19(b). After the fault cleared, the STATCOM prevents the electrical torque loss, by injecting sufficient amount of reactive power to the system. Consequently, the FSIG rotor speed start decreases and returns back to its initial value as shown in Figure 19(b). On comparing Figure 19(a) and (c), the real power supplied by FSIG varies exactly similar to its electrical torque.

Regarding the reactive power consumption of the FSIG during normal operating condition, it is drawing 4 Mvar from the grid whereas the rest that is, 1 Mvar is being supplied by the STATCOM. Just after the fault clearance, FSIG withdraws almost 20 Mvar from the grid but due to the corrective action taken by the STATCOM which suddenly pumps about 15 Mvar into PCC, the amount of reactive power drawn from the grid

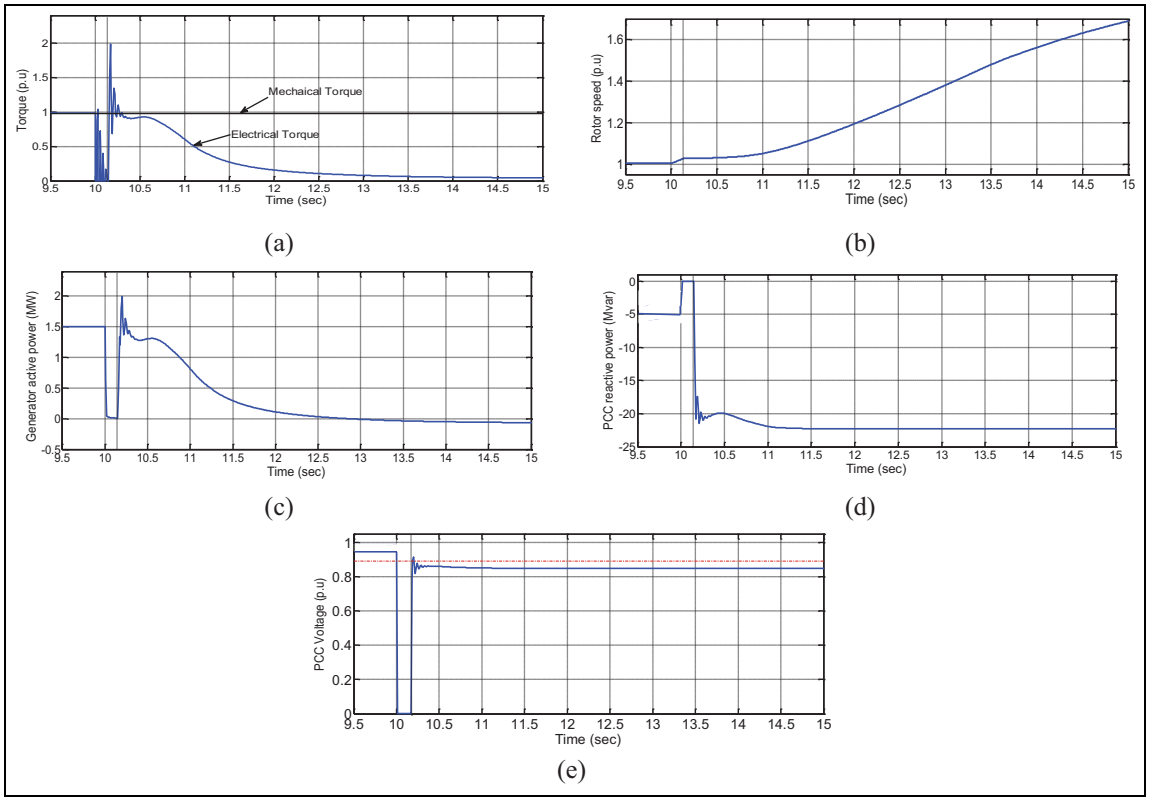

Figure 18. Simulation results without STATCOM and pitch angle controller: (a) electrical and mechanical torques of the generator, (b) generator rotor speed, (c) generator active power, (d) reactive power at the PCC, and (e) voltage at the PCC.

starts reducing. However due to the fault clearance, the grid itself is able to recover the PCC voltage and therefore, the reactive power supplied by STATCOM goes on reducing as observed from Figure 19(d) and (f). The simultaneous reactive support from the grid and the STATCOM restores the PCC voltage to its nominal value after 13 seconds as shown in Figure 19(e).

However, the voltage at PCC recovers to about 0.85 p.u just after the fault clearance. But, it takes time duration of 1.9 seconds to recover the voltage upto 0.9 p.u from the fault occurrence time, which does not meet the grid code requirement (see Figure 2). Therefore, STATCOM installment is able to improve the low voltage ride-through capability of the FSIG to some extent but, alone is not sufficient to meet the grid code requirement which provides the scope for further improvement of LVRT capability with the help of pitch-angle control of wind turbine as discussed earlier. Moreover, as observed from Figure 19(b) and (c), rotor speed and active power are not free from the oscillations, resulting in grid frequency problems (especially in case, large wind farms are connected to power system networks). These oscillations are also can be damped with the help of designed pitch-angle control scheme.

Case 3: System with STATCOM and pitch-angle control (i.e. UVPC)

As explained earlier, in order to further improve the LVRT capability of the wind farm, UVPC control strategy is used through which, a simultaneous control of STATCOM and pitch-angle control is achieved. During the network disturbances, the proposed strategy injects the justified amount of reactive power as required during rotor acceleration. Besides, it can vary the mechanical torque by changing the pitch (rotor blade) angle of the wind turbine. The simulation results obtained by employing the proposed UVPC strategy to the system are as shown in Figure 20(a) to (h).

It is observed from Figure 20(a) that during the fault, the pitch-angle control (as shown in Figure 20(g)) helps in reducing the mechanical torque from 1 to 0.825 p.u, which allows the rotor speed to reach only about 1.025 p.u as shown in Figure 20(f) but earlier, it was able to go beyond 1.025 p.u (see Figure 19(b)). As a result, the 0.9 p.u of

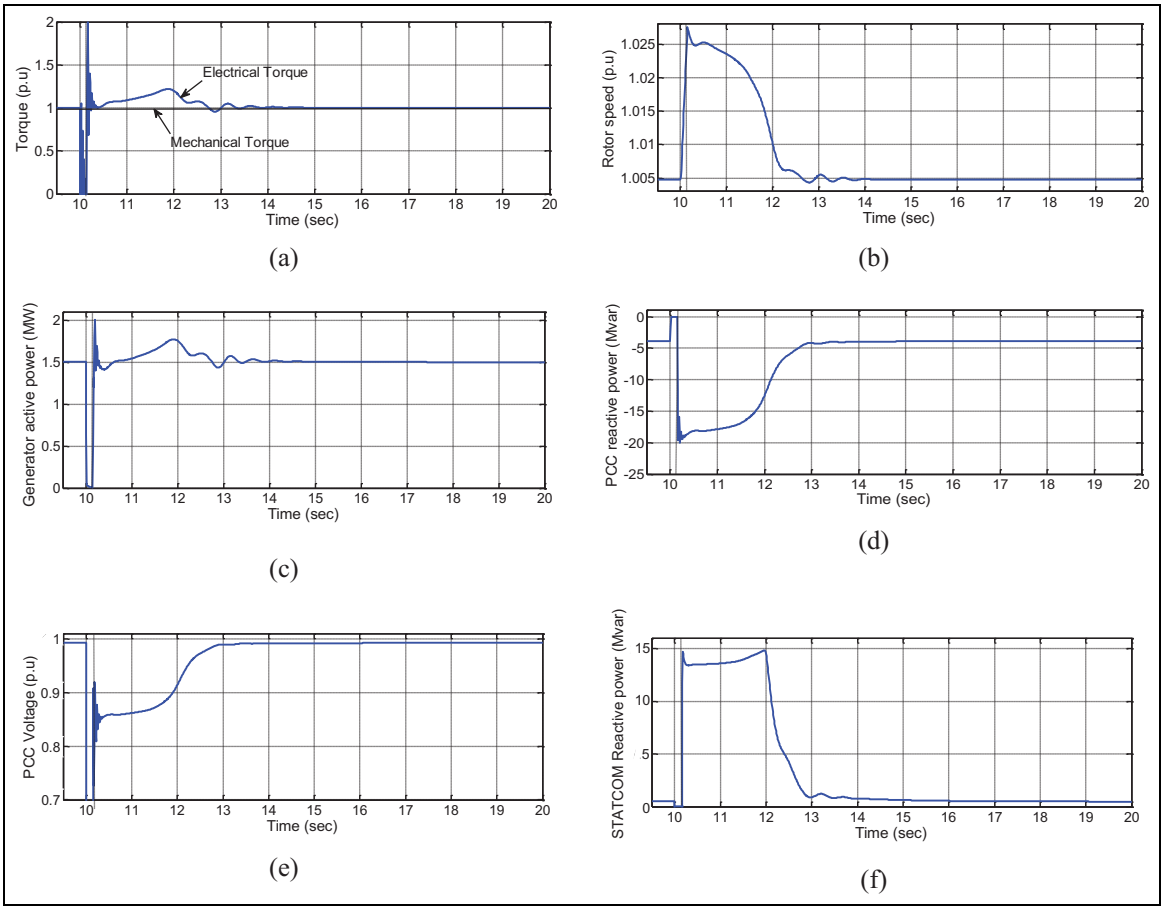

Figure 19. Simulation results with STATCOM: (a) electrical and mechanical torques of the generator, (b) generator rotor speed, (c) generator active power, (d) reactive power at the PCC, (e) voltage at the PCC, and (f) STATCOM reactive power injection.

PCC voltage recovery has been achieved with time duration of 1.4 seconds as shown in Figure 20(e) and satisfying the grid code, as compared to the previous case where voltage recovery of 0.9 p.u is achieved with time duration of 1.9 seconds. Therefore, the addition of STATCOM with pitch angle control (UVPC) can able to achieve the grid code requirements.

After the voltage recover (0.9 p.u), the pitch-angle control increases the mechanical torque which causes rotor speed to reduce and regain its initial value within 12 seconds whereas it was taking about 14 seconds (see Figure 19(b)). In addition, the pitch-angle control is able to remove the oscillations in the rotor speed. Similarly, if compare Figure 19(a) and (c) with Figure 20(b) and (c) respectively, there is no major difference but the pitch-angle control is effective in eliminating the oscillations in lesser time.

On comparing Figure 20(d) with Figure 19(d), it is observed that the pitch-angle control also contributes in reducing the reactive power drawn by the FSIG from the grid (after the fault clearance) from 20 to 16 Mvar. Even the reactive power contribution from the STATCOM (as shown in Figures 19(f) and 20(h)) reduce from about 15 to 13 Mvar and its duration also get reduced from 12 to 11.5 seconds, which indicates that pitch-angle control helps in reducing the size of STATCOM to be installed too.

The performance of the UVPC is also compared with respect to critical clearing time (CCT). For a given system, it is essential to find the maximum value of CCT (maximum fault duration) for which system remains in stable state. In this paper, CCT value is determined from the simulation in which, it is obtained by increasing the fault time interval for the same fault, until the system loses its stability. For example, simulation results in Figure 21 shows the rotor speed of the FSIG subjected to different faults durations with UVPC. The solid line represents rotor speed variation for 0.15 second fault and dotted line shows rotor speed variation for the maximum fault duration of 0.452 second. Since the CCT is increased, UVPC is able to increase the stability of the wind farm system.

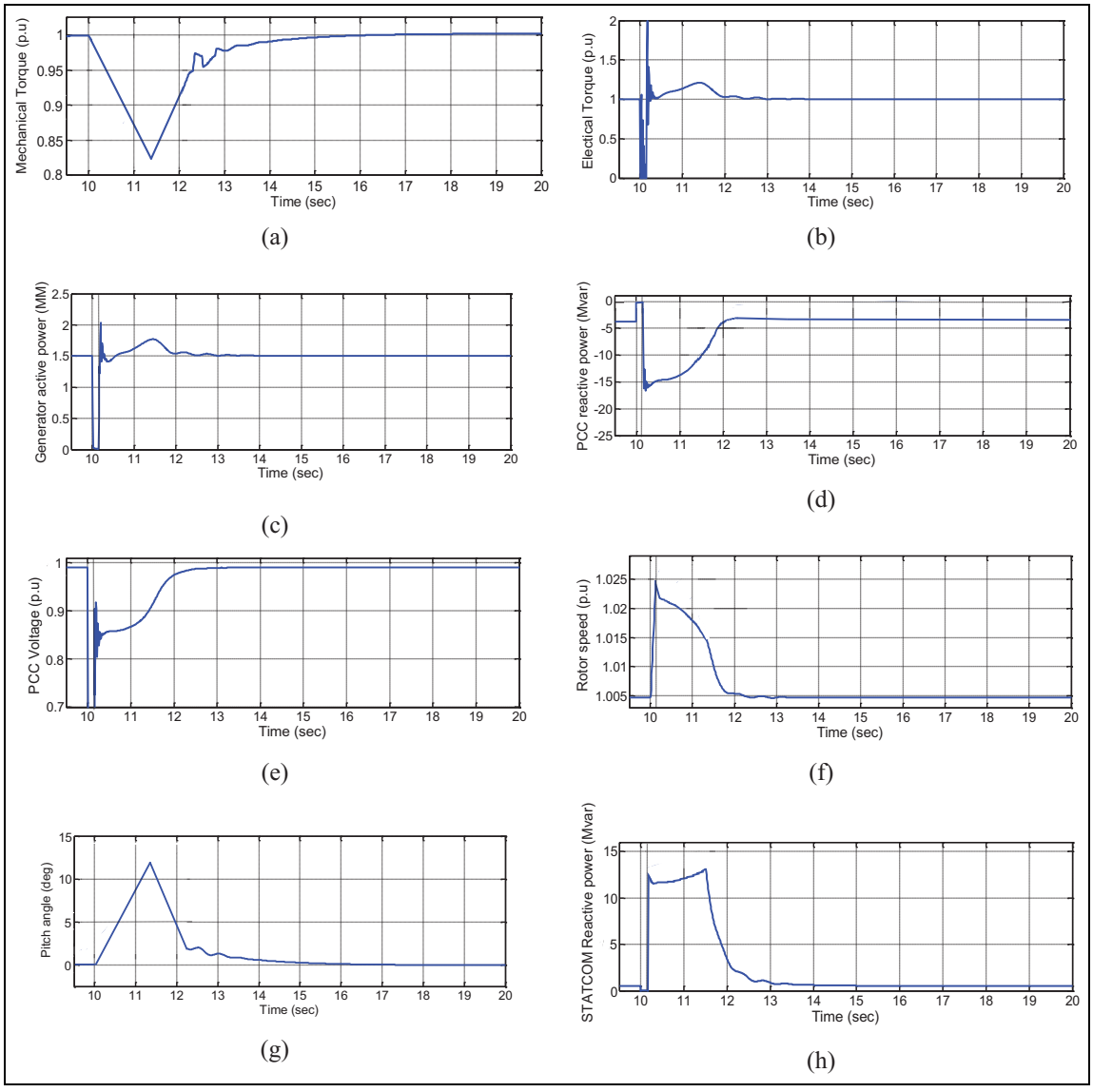

Figure 20. Simulation results with UVPC strategy: (a) mechanical torque of the generator, (b) electrical torque of the generator, (c) generator active power, (d) reactive power at the PCC, (e) voltage at the PCC, (f) generator rotor speed, (g) pitch-angle of the wind turbine, and (h) STATCOM reactive power injection.

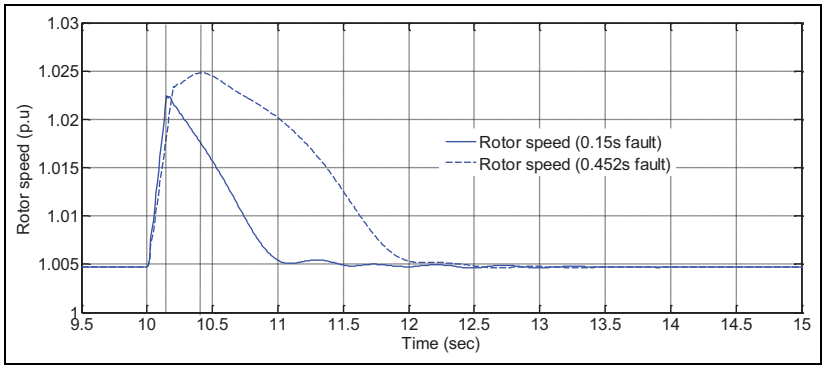

Figure 21. Rotor speed of generator with UVPC under different faults interval.

Table 2. Performance comparison.

STATCOM capacity (Mvar)	CCT(s) for the system with STATCOM	CCT(s) for the system with UVPC
15	0.445	0.452
20	0.503	0.513
25	0.521	0.543

In order to further investigate the applicability of the proposed UVPC controller, different STATCOM capacities are considered. Table 2 shows the controllers' performance comparison in terms of CCT with different STATCOM capacities. The CCT of the system with a 15 Mvar STATCOM is 0.452 second with UVPC strategy, compared with 0.445 second with STATCOM. Similar results are also obtained with 20 and 25 Mvar STATCOM. This shows that the proposed UVPC can provide increased CCT, which consequently enhances the LVRT capability.

Conclusions

In this work, UVPC control strategy is proposed to guarantee satisfying the LVRT grid code requirement. In this regard, static synchronous compensator (STATCOM) provides dynamic reactive power support to assist the fixed-speed induction generator for voltage restoration. Besides, the pitch-angle controller of constant speed wind turbines can effectively reduce the wind turbine mechanical power, preventing the wind generator from over-speeding. Therefore, using STATCOM in combination with pitch angle control, named as unified voltage and pitch-angle (UVPC) control strategy, enhances the LVRT capability of the fixed speed wind farm as well fulfilling the grid code requirement when it subjected to severe faults. In addition, the proposed UVPC helps in reducing the size of the STATCOM to be installed for improving the LVRT of such wind farms.

Declaration of conflicting interests

The author(s) declared no potential conflicts of interest with respect to the research, authorship, and/or publication of this article.

Funding

The author(s) received no financial support for the research, authorship, and/or publication of this article.

ORCID iD

Kanasottu Anil Naik https://orcid.org/0000-0002-3321-5097

References

Abdel-Baqi O and Nasiri A (2011) Series voltage compensation for DFIG wind turbine low-voltage ride-through solution. *IEEE Transactions on Energy Conversion* 26(1): 272–280.

Ackerman T (2005) *Wind Power in Power System*. Chichester: John Wiley & Sons. Ltd.

Chen WL and Hsu YY (2008) Unified voltage and pitch angle controller for wind-driven induction generator system. *IEEE Transactions on Aerospace and Electronic Systems* 44(3): 913–926.

De Mello F, Feltes J, Hannett L, et al. (1982) Application of induction generators in power system. *IEEE Transactions on Power Apparatus and Systems* PAS-101(9): 3385–3393.

Duong MQ, Grimaccia F, Leva S, et al. (2015) Hybrid controller for transient stability in wind generators. In: *IEEE Conference, Clemson university power systems conference (PSC)*, Clemson, USA, pp. 1–7. IEEE.

Grilo AP, Mota ADA, Mota LTM, et al. (2007) An analytical method for analysis of large-disturbance stability of induction generators. *IEEE Transactions on Power Systems* 22(4): 1861–1869.

Hagras H and Wagner C (2012) Towards the wide spread use of type-2 fuzzy logic systems in real world applications. *IEEE Computational Intelligence Magazine* 7: 14–24.

Karnik NN and Mendel JM (1999) Type-2 fuzzy logic systems. *IEEE Transactions on Fuzzy Systems* 7(6): 643–658.

Lima FK, Luna A, Rodriguez P, et al. (2010) Rotor voltage dynamics in the doubly fed induction generator during grid faults. *IEEE Transactions on Power Electronics* 25(1): 118–130.

Mendel JM (1999) Computing with words when words can mean different things to different people. In: *Int. ICSC congress computat intell: Methods applicat, 3rd annu symp fuzzy logic applicat*, pp.1–7. IEEE.

Mendel JM, John RI and Liu F (2006) Interval type-2 fuzzy logic systems made simple. *IEEE Transactions on Fuzzy Systems* 14(6): 808–821.

Mizumoto M and Tanaka K (1976) Some properties of fuzzy sets of type 2. *Information and Control* 31: 312–340.

Molinas M and Undeland T (2008) Low voltage ride through of wind farms with cage generators: STATCOM versus SVC. *IEEE Transactions on Power Electronics* 23(3): 1104–1117.

Muyeen SM, Ali MH, Takahashi R, et al. (2006) Transient stability analysis of grid connected wind turbine generator system considering multi-mass shaft modeling. *Electric Power Components and Systems* 34: 1121–1138.

Muyeen SM, Tamura J and Murata T (2009) *Stability augmentation of a grid connected wind farm*. London: Springer-Verlag Ltd.

Noureldeen O, Rihan M and Hasanin B (2011) Stability improvement of fixed speed induction generator wind farm using STATCOM during different fault locations and durations. *Ain Shams Engineering Journal* 2: 1–10.

Qilian L and Mendel JM (2000) Interval type-2 fuzzy logic systems: Theory and design. *IEEE Transactions on Fuzzy Systems* 8(5): 535–550.

Ramirez D, Martinez S, Blazquez F, et al. (2012) Use of STATCOM in wind farms with fixed-speed generators for grid code compliance. *Renewable Energy* 37: 202–212.

Rathi MR and Mohan N (2005) A novel robust low voltage and fault ride through for wind turbine application operating in weak grids. In: *IEEE industrial electronics society conference*, Raleigh, NC, pp.2481–2486. New York: IEEE.

Shima Y, Takahashi R, Murata T, et al. (2008) Transient stability simulation of wind generator expressed by two-mass model. *Electrical Engineering in Japan* 162(3): 27–37.

Singh B, Murthy SS and Gupta S (2006) STATCOM-Based voltage regulator for self-excited induction generator feeding non-linear loads. *IEEE Transactions on Industrial Electronics* 53(5): 1437–1452.

Singh G and Sundaram K (2021a) Common mode current effects and challenges for wind turbine generator application. In: *ASME power conference*, July, 85109, p.V001T09A002. American Society of Mechanical Engineers.

Singh G and Sundaram K (2021b) Manufacturing deformation impact on the performance of electrical generator for the wind turbine application. *Wind Engineering* 45(5): 1193–1205.

Singh G and Sundaram K (2022) Methods to improve wind turbine generator bearing temperature imbalance for onshore wind turbines. *Wind Engineering* 46: 150–159.

Singh G, Lentijo S and Sundaram K (2019a) The impact of the converter on the reliability of a wind turbine generator. In: *ASME power conference*, July, 59100, p.V001T06A016. American Society of Mechanical Engineers.

Singh G, Matuonto M and Sundaram K (2019b) Impact of imbalanced wind turbine generator cooling on reliability. In: *2019 10th international renewable energy congress (IREC)*, March, pp.1–6. New York: IEEE.

Singh G, Sundaram K and Saleh A (2019c) Addressing reduced ingress protection class & proper filter selection for open ventilated (IC3A1) wind turbine generator. In: *2019 10th international renewable energy congress (IREC)*, March, pp.1–5. New York: IEEE.

Singh G, Sundaram K and Matuonto M (2021) A solution to reduce overheating and increase wind turbine systems availability. *Wind Engineering* 45(3): 491–504.

Singh G, Matuonto M, Amos J, et al. (2019d) System of systems strand tilt analysis perspective on MediuMHigh voltage stator bar and a non-destructive testing case study. In: *2019 IEEE international systems conference (SysCon)*, April, pp.1–8. New York: IEEE.

Singh G, Saleh A, Amos J, et al. (2018) Ic6a1a6 vs. Ic3a1 squirrel cage induction generator cooling configuration challenges and advantages for wind turbine application. In: *ASME power conference*, Lake Buena Vista, Florida, USA, June, 51395, p.V001T06A002. American Society of Mechanical Engineers.

Strzelecki R and Benysek G (2008) *Power Electronics in Smart Electrical Energy Networks*. London: Springer.

Suul JA, Molinas M and Undeland T (2010) STATCOM-based indirect torque control of induction machines during voltage recovery after grid faults. *IEEE Transactions on Power Electronics* 25(5): 1240–1250.

Tamura J (2001) Transient stability simulation of power system including wind generator by PSCAD/EMTDC. In: *IEEE porto power tech proceedings*; 4: p.EMT–108. New York: IEEE.

Tan OT, Paap GC and Kolluru MS (1993) Thyristor-controlled voltage regulators for critical induction motor loads during voltage disturbances. *IEEE Transactions on Energy Conversion* 8(1): 100–106.

The Global Wind Energy Council Belgium (2022). Available at: https://gwec.net/global-wind-report-2022/ (accessed 14 August 2020).

Thet AK and Saitoh H (2009) Pitch control for improving the low-voltage ride-through of wind farm. In: *Transmission & distribution conference & exposition: Asia and Pacific*, Seoul, South Korea, pp.1–4. New York, NY: IEEE.

The Wind Power (2015). Available at: http://www.thewindpower.net/windfarm_en_86_challicum-hills.php (accessed 5 May 2017).

Trudnowski DJ, Gentile A, Khan JM, et al. (2004) Fixed-speed wind-generator and wind-park modeling for transient stability studies. *IEEE Transactions on Power Systems* 19(4): 1911–1917.

Wu B, Lang Y, Zargari N, et al. (2011) *Power Conversion and Control of Wind Energy Systems*. Chichester: John Wiley & Sons. Ltd.

Zhang J, Yin Z, Xiao X, et al. (2009) Enhancement voltage stability of wind farm access to power grid by novel SVC. In: *IEEE conference on industrial electronics and applications*, Xian, China, pp.2262–2266. New York: IEEE.

Zhu W and Cao RF (2009) Improved low voltage ride-through of wind farm using STATCOM and pitch control. In: *IEEE 6th international power electronics and motion control conference*, Wuhan, China, pp.2217–2221. New York: IEEE.